Possibility to synthesize $Z > 118$ superheavy nuclei with ^{54}Cr projectiles

Jia-Xing Li (李佳星) and Hong-Fei Zhang (张鸿飞) *

School of Physics, Xi'an Jiaotong University, 710049 Xi'an, People's Republic of China
and School of Nuclear Science and Technology, Lanzhou University, 730000 Lanzhou, People's Republic of China

(Received 1 August 2023; accepted 13 September 2023; published 6 October 2023)

The capture and evaporation residue cross sections (ERCSs) for heavy ion fusion reactions are calculated by using the dinuclear system model. The calculation results are in good agreement with the experimental data of reactions ^{48}Ca + ^{244}Pu and ^{48}Ca + ^{248}Cm. To investigate the possibility of synthesizing superheavy nuclei (SHN) with $Z > 118$ using the ^{54}Cr projectile, a comparative analysis is conducted between the ERCSs obtained with ^{48}Ca and ^{54}Cr projectiles for the synthesis of SHN with $Z = 114$–118. The analysis further investigates the variation trends of ERCSs, capture cross sections, fusion probabilities, and survival probabilities with an increasing compound nucleus proton number (Z_{CN}). Furthermore, we predict the ERCSs for the synthesis of new elements $Z = 119$, $Z = 120$, $Z = 121$, and $Z = 122$ through the reactions ^{54}Cr + ^{243}Am, ^{54}Cr + ^{248}Cm, ^{54}Cr + ^{249}Bk, and ^{54}Cr + ^{249}Cf, respectively. However, the obtained results fall below the detectable limits of currently available facilities. Thus, to successfully synthesize SHN with $Z > 118$, experimental efforts must focus on increasing the beam intensity and improving separation and detection techniques.

DOI: 10.1103/PhysRevC.108.044604

I. INTRODUCTION

In modern nuclear physics, the synthesis of superheavy nuclei (SHN) is one of the main research topics due to the great motivation of searching for the limit of elements [1]. Currently, 118 elements have been discovered, and the seventh period of the periodic table has been filled. It is worth mentioning that the experiments of discovering elements $Z = 114$–118 all used ^{48}Ca projectiles [2–5]. For these ^{48}Ca-induced fusion reactions, a lot of theoretical investigations have been carried out, with two main purposes: the first reason is to find out and analyze the synthesis mechanism of SHN, the second one is to search for the best projectile-target combination and a suitable incident energy to guide the synthesis experiment of new SHN and their isotopes [6]. Due to the lack of appropriate targets heavier than ^{249}Cf, this circumstance causes extreme difficulties in experiments of the synthesis of SHN with $Z > 118$, so we can only rely on projectiles heavier than ^{48}Ca [7]. Several recent studies indicate that ^{54}Cr shows promise as a projectile for use in experiments aimed at synthesizing new elements [8–10]. Thus, a systematic investigation of fusion-evaporation reactions using the ^{54}Cr projectile and analyzing the possibility for synthesizing SHN with $Z > 118$ using the ^{54}Cr projectile are essential and necessary.

Experimentally, attempts have been made to synthesize superheavy nuclei with $Z > 118$ through reactions such as ^{244}Pu + ^{58}Fe [11], ^{249}Bk + ^{50}Ti [12], ^{249}Cf + ^{50}Ti [12], and ^{238}U + ^{64}Ni [13]. However, these new elements have not been discovered yet. In heavy-ion synthesis experiments, the choice of projectile-target combination significantly influences the cross sections, and the beam energy also plays a crucial role in determining the reaction outcomes. Even small variations of a few MeV in the beam energy can lead to orders of magnitude changes in the cross sections [7,14,15]. Additionally, the cross sections for the synthesis of elements with $Z > 118$ are extremely low, approaching the current detection efficiency limits of available detectors. Consequently, to successfully synthesize elements with $Z > 118$ in experiments, it is essential not only to identify suitable projectile-target combinations and precise beam energies theoretically but also to enhance key techniques such as improving detection efficiency.

Theoretically, many models have been developed to describe the evaporation residue cross sections (ERCSs) of fusion reactions [16–19]. When it comes to SHN synthesis with $Z > 118$, theorists have actively explored based on different models [8,10]. In this study, we employ the dinuclear system (DNS) model to calculate the ERCSs of fusion reactions. Based on the concept of the DNS model [20–25], the ERCSs are jointly determined by capture section, fusion probability, and survival probability. The capture cross section is calculated with an empirical coupled-channel model and the survival probability of the formed compound nucleus is calculated with a statistic model. The fusion probability is obtained by solving the sum of the solutions of the transport master equation that distinguishes protons and neutrons.

Motivated by the urgent need to expand the periodic table and explore the limits of element existence, as well as the strong drive to potentially synthesize superheavy nuclei with $Z > 118$ using the ^{54}Cr projectile, we conducted a systematic study on fusion reactions to produce a series of SHN. We compared their ERCSs with those induced by ^{48}Ca fusion reactions. Additionally, we investigated the trends of ERCSs, capture cross sections, fusion probabilities, and survival probabilities as the Z_{CN} increased. Moreover, we predicted the ERCSs for $Z = 119$, $Z = 120$, $Z = 121$, and $Z = 122$

*zhanghf@xjtu.edu.cn

nuclei synthesized using ^{54}Cr projectile. Our research aims to explore the synthesis mechanisms of SHN using the ^{54}Cr projectile and analyze the possibility for synthesizing SHN $Z > 118$ with ^{54}Cr.

II. THEORETICAL FRAMEWORK

The DNS model postulates that the compound system is formed through a sequence of nucleon or cluster transfers from the light nucleus to the heavy one in a touching configuration [26]. The ERCS is commonly expressed as a summation over all partial waves J at the center-of-mass energy $E_{\mathrm{c.m.}}$ [27]:

$$\sigma_{ER}(E_{\mathrm{c.m.}}) = \frac{\pi\hbar^2}{2\mu E_{\mathrm{c.m.}}}\sum_J (2J+1)T(E_{\mathrm{c.m.}}, J) \times P_{CN}(E_{\mathrm{c.m.}}, J)\times W_{\mathrm{sur}}(E_{\mathrm{c.m.}}, J). \quad (1)$$

Here, $T(E_{\mathrm{c.m.}}, J)$ is the transmission probability of the two colliding nuclei overcoming the Coulomb potential barrier to form a dinuclear system, $P_{CN}(E_{\mathrm{c.m.}}, J)$ is the fusion probability. $W_{\mathrm{sur}}(E_{\mathrm{c.m.}}, J)$ is the survival probability.

The empirical coupled channel model [28,29] is employed to calculate the capture cross section of two colliding nuclei. The transmission probability is estimated using the barrier distribution function method, where the function is assumed to follow an asymmetric Gaussian distribution form. The capture cross section can be written as [30]

$$\sigma_{cap}(E_{\mathrm{c.m.}}) = \frac{\pi\hbar^2}{2\mu E_{\mathrm{c.m.}}}\sum_J (2J+1)T(E_{\mathrm{c.m.}}, J), \quad (2)$$

the transmission probability $T(E_{\mathrm{c.m.}}, J)$ can be calculated by the Hill-Wheeler formula [31]. Considering the coupling channel effect through the potential barrier distribution function, the transmission probability can be written as

$$T(E_{\mathrm{c.m.}}, J) = \int f(B)T(E_{\mathrm{c.m.}}, J)dB, \quad (3)$$

the barrier distribution function is taken as asymmetric Gaussian form

$$f(B) = \begin{cases} \frac{1}{N}\exp\left[-\left(\frac{B-B_m}{\Delta_1}\right)^2\right] & B < B_m \\ \frac{1}{N}\exp\left[-\left(\frac{B-B_m}{\Delta_2}\right)^2\right] & B > B_m \end{cases}. \quad (4)$$

Here, $B_m = \frac{B_s+B_0}{2}$, B_0 is the height of the Coulomb barrier at waist-to-waist orientation, and B_s is the minimum height of the Coulomb barrier with variance of dynamical deformation β_1 and β_2, N is the normalization constant. $\Delta_2 = (B_0 - B_s)/2$. The value of Δ_1 is usually 2–4 MeV less than the value of Δ_2 [32], and in this article, we take a value of 2 MeV. Considering the quadrupole deformation, the nucleus-nucleus interaction potential can be written as

$$\begin{aligned} &V(r, \beta_1, \beta_2, \theta_1, \theta_2) \\ &= V_C(r, \beta_1, \beta_2, \theta_1, \theta_2) + V_N(r, \beta_1, \beta_2, \theta_1, \theta_2) \\ &\quad + \tfrac{1}{2}C_1\left(\beta_1 - \beta_1^0\right)^2 + \tfrac{1}{2}C_2\left(\beta_2 - \beta_2^0\right)^2. \end{aligned} \quad (5)$$

Here, $\beta_1(\beta_2)$ is the parameter of dynamical quadrupole deformation for projectile (target). $\beta_1^0(\beta_2^0)$ is the parameter of static deformation for projectile (target). $\theta_1(\theta_2)$ is the angle between radius vector $\vec{r}$ and the symmetry axes of statically deformed projectile (target). $C_{1,2}$ are the stiffness parameters of the nuclear surface, which are calculated with the liquid drop model [33]. We take the Coulomb potential $V_C(r, \beta_1, \beta_2, \theta_1, \theta_2)$ and nuclear potential $V_N(r, \beta_1, \beta_2, \theta_1, \theta_2)$ mentioned in Ref. [30].

The $P_{CN}(E_{\mathrm{c.m.}}, J)$ is the probability of the evolution of the system from the contact configuration to the formation of the compound nucleus. The time evolution of the distribution probability function, $P(Z_1, N_1, E_1, t)$ can be obtained by solving the master equation in the corresponding potential energy surface [35]. The fusion probability of the DNS is given by

$$P_{CN}(E_{\mathrm{c.m.}}, J) = \sum_{Z_1=1}^{Z_{BG}}\sum_{N_1=1}^{N_{BG}} P(Z_1, N_1, E_1, \tau_{\mathrm{int}}), \quad (6)$$

the N_{BG} and Z_{BG} are the neutron number and charge number at the Businaro-Gallone point, respectively. The interaction time τ_{int} is obtained by the deflection function method [36]. The survival probability of emitting x_n neutrons can be written as

$$W_{\mathrm{sur}}(E_{\mathrm{c.m.}}, x, J) = P(E_{CN}^*, x, J)\prod_{i=1}^{x}\left[\frac{\Gamma_n}{\Gamma_n + \Gamma_f}\right]_i. \quad (7)$$

In the formula, E_{CN}^* represents the excitation energy of the compound nuclei. $P(E_{CN}^*, x, J)$ is the realization probability of emitting x neutrons, which is addressed in detail in Ref. [37]. Γ_n and Γ_f represent the partial wave decay width of evaporating neutron and fission, respectively [38]. E_i^* represents the excitation energy of the ith neutron before evaporation,

$$E_{i+1}^* - B_i^n - 2T_i. \quad (8)$$

Here, B_i^n is the separation energy of the ith neutron, T_i is the nuclear temperature before evaporating the ith neutron. In this work, the fission barrier before evaporating the ith neutron is obtained by

$$B_i^f = B_i^f(E_i^* = 0)\exp\left(-E_i^*/E_d\right), \quad (9)$$

the shell correction energy $B_i^f(E_i^* = 0)$ is taken from Ref. [39]. E_d is the damping factor, and its expression can be written as

$$E_D = 5.48A^{1/3}/(1 + 1.3A^{-1/3}). \quad (10)$$

III. RESULTS AND DISCUSSION

Based on the DNS model, we have provided the capture cross sections and ERCSs of ^{48}Ca induced reactions with target nuclei ^{244}Pu and ^{248}Cm, and compared them with the available experimental data in Fig. 1. It can be clearly seen that the capture cross sections and ERCSs are well consistent with the experimental data. Since both capture cross section and ERCS can match the experimental values well, it can be inferred that the product of fusion probability and survival probability calculated by the DNS model is reasonable. These results give us confidence in studying the fusion evaporation

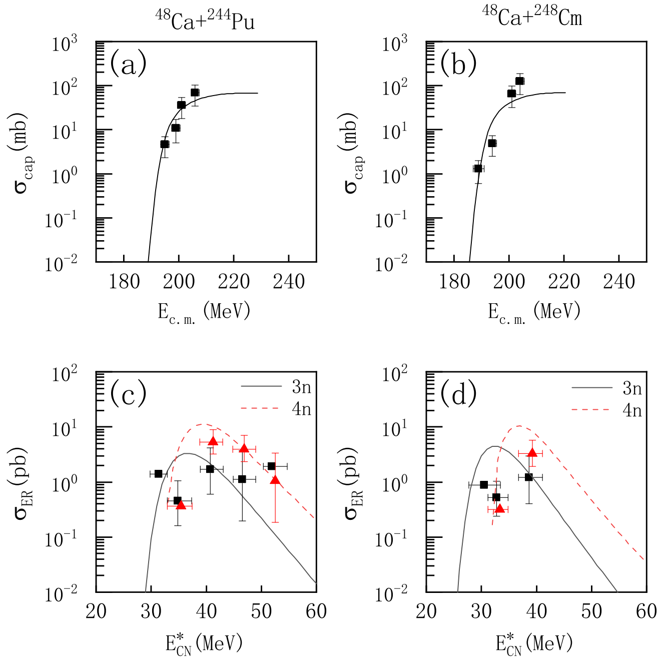

FIG. 1. The capture cross sections of ^{48}Ca induced reactions with target nuclei ^{244}Pu (a) and ^{248}Cm (b). The ERCSs of ^{48}Ca induced reactions with target nuclei ^{244}Pu (c) and ^{248}Cm (d) The experimental data of the capture cross sections are taken from Ref. [34]. The experimental data of ERCSs are taken from Ref. [2], where the experimental data of $3n$ and $4n$ channels are represented by black squares and red triangles, respectively.

reaction induced by ^{54}Cr, which is heavier than ^{48}Ca, and may be a promising approach for synthesizing new superheavy nuclei with $Z > 118$. In the current DNS model, experimental data can be reasonably reproduced, but the simple consistency between theoretical results and experimental data is not sufficient to reveal the essential substances of the phenomena involved [40]. The ERCS is determined by the product of capture cross section, fusion probability, and survival probability, and in fact, all theoretical models provide an approximate product of the three. In general, the capture cross sections are nearly the same, the difference between various models lies in the fusion probability, and survival probability. The physical considerations of various models are different, and the calculation results of the fusion probability are quite different, even one order of magnitude [41]. The survival probability is very sensitive to parameters, such as fission barrier and neutron separation energy, as well as some empirical parameters of the model itself. However, the calculated ERCSs of various models can conform to the experimental results, because the fusion probability and survival probability are mutually compensated [42].

In Fig. 2, we present the maximum ERCSs as a function of the $Z_{\rm CN}$. One can see that regardless of whether ^{48}Ca or ^{54}Cr is used as the projectile nucleus, both exhibit a similar decreasing trend in the maximum ERCS as compound nucleus proton number increases. Notably, when ^{48}Ca is replaced by ^{54}Cr as the projectile, leading to the formation of compound nuclei with the same proton number, the maximum ERCS

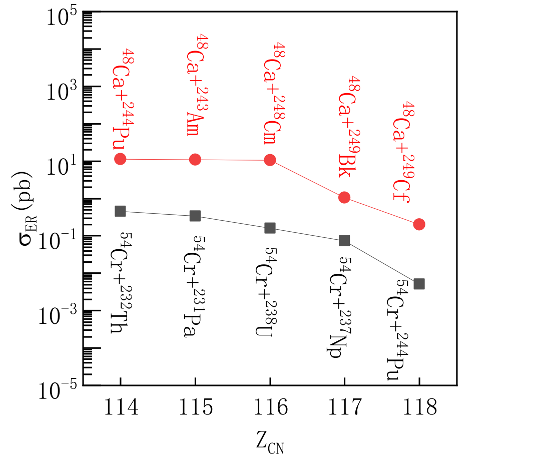

FIG. 2. The maximum ERCSs as a function of $Z_{\rm CN}$ for synthesizing SHN with $Z = 114$–118 using ^{48}Ca and ^{54}Cr, respectively.

decreases by approximately 1–2 orders of magnitude. This observation indicates the sensitivity of ERCS to the selection of projectile nucleus.

In the aforementioned study, we analyzed the ERCSs ^{54}Cr + ^{232}Th, ^{54}Cr + ^{231}Pa, ^{54}Cr + ^{238}U, ^{54}Cr + ^{237}Np, and ^{54}Cr + ^{244}Pu. To gain a clearer understanding of the reaction mechanism induced by ^{54}Cr, we also need to analyze their capture cross sections, survival probabilities, and fusion probabilities. In Fig. 3, we present the capture cross sections for the aforementioned five reactions. It can be observed that reaction ^{54}Cr + ^{232}Th has the highest capture cross section, and as the $Z_{\rm CN}$ increases, the capture cross section shows a decreasing trend. When the $E_{\rm c.m.}$ exceeds 240 MeV, the differences in capture cross sections between these reactions become small. In heavy-ion fusion reactions, the competition between the long-range repulsive Coulomb interaction and the short-range attractive nuclear force leads to the formation of a interaction potential "pocket". The capture cross section depends on the

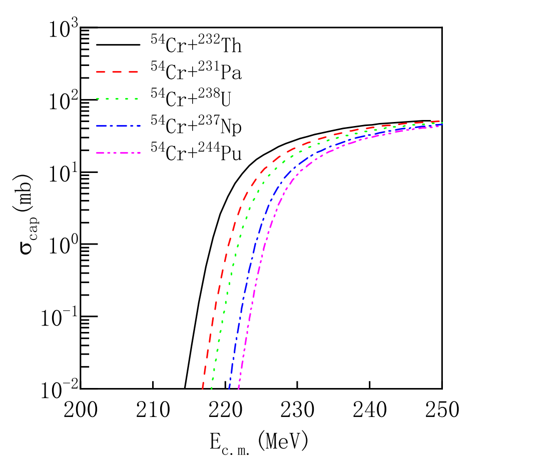

FIG. 3. The capture cross sections of the fusion reactions ^{54}Cr + ^{232}Th, ^{54}Cr + ^{231}Pa, ^{54}Cr + ^{238}U, ^{54}Cr + ^{237}Np, and ^{54}Cr + ^{244}Pu used for the synthesis of SHN $Z = 114$–118, using ^{54}Cr as the projectile nucleus.

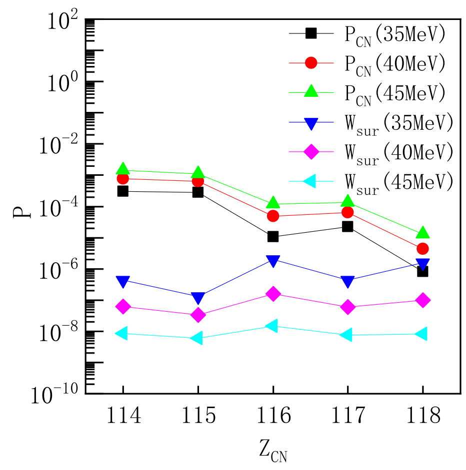

FIG. 4. The fusion probabilities of compound nuclei with $Z = 114–118$ at excitation energies of 35 MeV, 40 MeV, and 45 MeV, as well as the survival probabilities for the $3n$ evaporation channel at the same excitation energies.

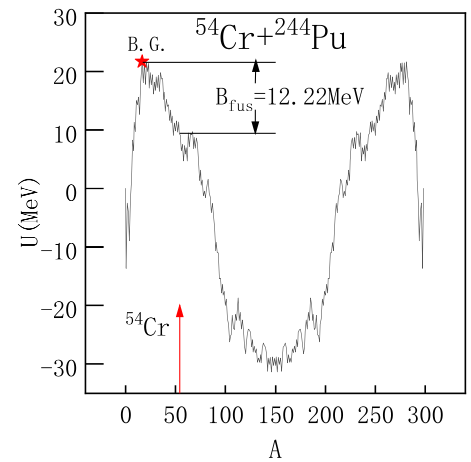

FIG. 5. The potential energy surface for the reaction $^{54}Cr + {}^{244}Pu$, the arrow in the figure indicates the entrance channel.

height and width of this pocket, as well as the coupling between relative motion and internal degrees of freedom.

In Fig. 4, we present the fusion probabilities of compound nuclei with $Z = 114–118$ at excitation energies of 35 MeV, 40 MeV, and 45 MeV, as well as the survival probabilities for the $3n$ evaporation channel at the same excitation energies. One can observe that, for the same fusion reaction, the fusion probability increases with the increase in excitation energy. This is because high excitation energies in the dinuclear system lead to significant energy dissipation, making it easier to overcome the inner fusion barrier B_{fus} and form compound nuclei. Similarly, one also can notice that the survival probability decreases with decreasing excitation energy, as higher excitation energies can disrupt the stability of the compound nuclei. Additionally, we can see that at the same excitation energy, the fusion probabilities generally show a decreasing trend with increasing Z_{CN}, especially between $Z = 115–116$ and $Z = 117–118$. Moreover, at the same excitation energy, the survival probabilities for the $3n$ evaporation channel exhibit evident odd-even effects, with the survival probabilities for even-Z compound nuclei being higher compared to their neighboring odd-Z counterparts.

According to the previous analysis, under the same excitation energy, the fusion probability generally decreases with the increase of Z_{CN}, and the fusion probability of the reaction $^{54}Cr + {}^{244}Pu$ synthesizing SHN $Z = 118$ is relatively small. Based on the DNS model, the calculation of fusion probability depends on the details of the potential energy surface. In Fig. 5, the potential energy surface for the reaction $^{54}Cr + {}^{244}Pu$ is displayed. The hindrance in the diffusion process by nucleon transfer to form the compound nucleus is the B_{fus}, which is defined as the difference of the driving potential at the Businaro-Gallone (B.G.) point and at the entrance position. In other words, in order to occur a fusion reaction, the dinuclear system must overcome this potential barrier. The smaller the internal fusion barrier, the more conducive to the formation of compound nucleus. We can clearly see in Fig. 5 that the B_{fus} of the reaction $^{54}Cr + {}^{244}Pu$ is 12.22 MeV, which is not conducive to the formation of compound nucleus and decreases the fusion probability of synthetic SHN.

In Fig. 6, we present the B_{fus} heights for compound nuclei $Z = 112–118$, as well as the fission barrier heights and neutron separation energies for the $3n$ evaporation channel. It can be observed that with an increase in Z_{CN}, the B_{fus} height shows an increasing trend, especially between $Z = 115–116$ and $Z = 117–118$. This is consistent with the decreasing fusion probabilities observed in Fig. 4 for $Z = 115–116$ and $Z = 117–118$. Furthermore, one can observe the variations in fission barriers and neutron separation energies. Lower neutron separation energies and higher fission barriers are favorable for the survival of compound nuclei. Figure 6 shows that even-Z compound nuclei have lower neutron separation energies and higher fission barriers, which explains their relatively higher survival probabilities observed in Fig. 4. It is worth mentioning that the choice of fission barriers and neutron separation energies is crucial for calculating survival probabilities. A 1 MeV change in the fission

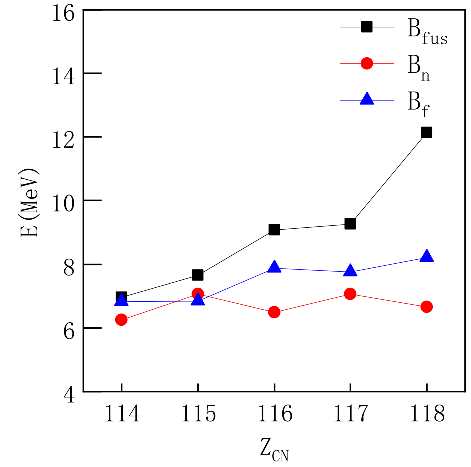

FIG. 6. Inner fusion barriers B_{fus} for $Z = 114–118$ compound nuclei using ^{54}Cr projectile, and fission barriers B_f and neutron separation energies B_n for the $3n$ evaporation channel.

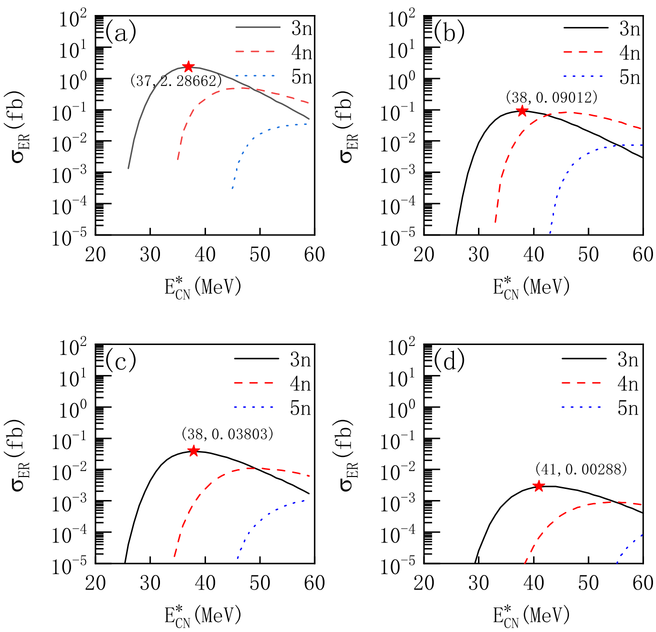

FIG. 7. The ERCSs for synthesizing SHN (a) $Z = 119$, (b) $Z = 120$, (c) $Z = 121$, and (d) $Z = 122$ through reactions $^{54}Cr + ^{243}Am$, $^{54}Cr + ^{248}Cm$, $^{54}Cr + ^{249}Bk$, and $^{54}Cr + ^{249}Cf$. The calculated values for $3n$, $4n$, and $5n$ channels are represented by black solid lines, red dashes, and blue dotted lines, respectively.

barrier can lead to a significant variation in the survival probabilities. However, currently all theoretical models have uncertainty in calculating the fission barrier of unknown superheavy nuclei [43]. After analyzing the synthesis of SHN $Z = 114$–118 using ^{54}Cr as the projectile, we conducted a study on the possibility of synthesizing superheavy nuclei $Z > 118$ using ^{54}Cr as the projectile. In Fig. 7, we present the ERCSs for synthesizing SHN $Z = 119$, $Z = 120$, $Z = 121$, and $Z = 122$ through reactions $^{54}Cr + ^{243}Am$, $^{54}Cr + ^{248}Cm$, $^{54}Cr + ^{249}Bk$, and $^{54}Cr + ^{249}Cf$. The maximum ERCS for $Z = 119$ is 2.28662 fb, for $Z = 120$ is 0.09012 fb, for $Z = 121$ is 0.03803 fb, and for $Z = 122$ is 0.00288 fb. As mentioned earlier, the maximum ERCS shows a decreasing trend with an increase in the Z_{CN}. Unfortunately, these ERCSs are lower than the limits currently achievable with experimental techniques (greater than 0.1 pb [44]). Therefore, synthesizing SHN with $Z > 118$ would require increasing beam intensity, improving detection techniques, and implementing efficient separation methods. Finally, we present in Table I the important physical parameters used in all the calculations mentioned above, including ground state nuclear quadrupole deformation β_2, binding energy of compound nucleus E_{CN}, reaction energy Q, single neutron separation energy of compound nucleus B_n, and fission barrier height of compound nucleus B_f.

IV. SUMMARY

In summary, the DNS model results demonstrate good agreement with the experimental outcomes for the capture cross sections and ERCSs of reactions $^{48}Ca + ^{244}Pu$ and $^{48}Ca + ^{248}Cm$. To gain insights into the synthesis mechanism of SHN using ^{54}Cr as the projectile, we conduct a detailed study on the fusion reaction for creating SHN with $Z = 114$–118. Replacing ^{48}Ca with ^{54}Cr as the projectile results in a significant decrease in the maximum ERCS for synthesizing compound nuclei with the same proton number, with a reduction of approximately 1–2 orders of magnitude. Furthermore, we perform a systematic analysis of fusion probabilities and survival probabilities at a given excitation energy. The findings indicate that fusion probabilities generally decrease with an increase in Z_{CN}, while survival probabilities show an odd-even variation with Z_{CN}. Moreover, we explore the possibility of synthesizing SHN with $Z > 118$ using ^{54}Cr. The calculated ERCSs for synthesizing $Z = 119$, $Z = 120$, $Z = 121$, and $Z = 122$ are found to be 2.28662 fb, 0.09012 fb, 0.03803 fb, and 0.00288 fb, respectively. These results appear to be lower than the detectable limits of currently available facilities. Therefore, achieving the synthesis of SHN with

TABLE I. Important input parameters for ERCS calculation in fusion-evaporation reactions, including ground state nuclear quadrupole deformation β_2, binding energy of compound nucleus E_{CN}, reaction energy Q, single neutron separation energy of compound nucleus B_n, and fission barrier height of compound nucleus B_f.

reactions	β_2(projectile)	β_2(target)	E_{CN}(MeV)	Q(MeV)	B_n(MeV)	B_f(MeV)
$^{48}Ca + ^{244}Pu$	0.00	0.237	2091.52	−160.44	7.05	8.68
$^{48}Ca + ^{243}Am$	0.00	0.237	2080.43	−164.98	7.33	8.55
$^{48}Ca + ^{248}Cm$	0.00	0.250	2108.64	−168.57	6.74	8.32
$^{48}Ca + ^{249}Bk$	0.00	0.250	2109.89	−170.07	6.77	8.31
$^{48}Ca + ^{249}Cf$	0.00	0.250	2105.02	−174.18	5.90	8.01
$^{54}Cr + ^{232}Th$	0.161	0.205	2051.93	−188.35	7.57	7.24
$^{54}Cr + ^{231}Pa$	0.161	0.195	2038.81	−194.44	7.87	7.40
$^{54}Cr + ^{238}U$	0.161	0.236	2083.10	−192.44	7.71	8.30
$^{54}Cr + ^{237}Np$	0.161	0.226	2069.62	−199.29	7.66	7.99
$^{54}Cr + ^{244}Pu$	0.161	0.237	2112.03	−198.35	7.01	7.61
$^{54}Cr + ^{243}Am$	0.161	0.237	2099.17	−204.65	7.71	7.81
$^{54}Cr + ^{248}Cm$	0.161	0.250	2126.77	−206.85	7.07	6.29
$^{54}Cr + ^{249}Bk$	0.161	0.250	2126.59	−211.78	7.04	6.00
$^{54}Cr + ^{249}Cf$	0.161	0.250	2120.06	−217.55	6.37	5.66

$Z > 118$ would require increasing beam intensity, enhancing detection techniques, and implementing efficient separation methods. We hope that the results and discussions presented in this paper provide valuable insights and support for experimental efforts in the synthesis of new elements.

ACKNOWLEDGMENTS

We are grateful to Prof. J. Q. Li, Z. Z. Ren, F. S. Zhang, S. G. Zhou, Z. G. Gan, and Z. Y. Zhang for valuable discussions. This work is supported by National Natural Science Foundation of China (Grants No. 12175170, 11675066.)

[1] S. Hofmann and G. Münzenberg, Rev. Mod. Phys. **72**, 733 (2000).
[2] Y. T. Oganessian, V. K. Utyonkov, Y. V. Lobanov, F. S. Abdullin, A. N. Polyakov, I. V. Shirokovsky, Y. S. Tsyganov, G. G. Gulbekian, S. L. Bogomolov, B. N. Gikal, A. N. Mezentsev, S. Iliev, V. G. Subbotin, A. M. Sukhov, A. A. Voinov, G. V. Buklanov, K. Subotic, V. I. Zagrebaev, M. G. Itkis, J. B. Patin, J. F. Wild, M. A. Stoyer, N. J. Stoyer, D. A. Shaughnessy, J. M. Kenneally, P. A. Wilk, R. W. Lougheed, R. I. Ilkaev, and S. P. Vesnovskii, Phys. Rev. C **69**, 054607 (2004).
[3] Y. T. Oganessian, F. S. Abdullin, S. N. Dmitriev, J. M. Gostic, J. H. Hamilton, R. A. Henderson, M. G. Itkis, K. J. Moody, A. N. Polyakov, A. V. Ramayya, J. B. Roberto, K. P. Rykaczewski, R. N. Sagaidak, D. A. Shaughnessy, I. V. Shirokovsky, M. A. Stoyer, N. J. Stoyer, V. G. Subbotin, A. M. Sukhov, Y. S. Tsyganov *et al.*, Phys. Rev. C **87**, 014302 (2013).
[4] Y. T. Oganessian, V. K. Utyonkov, Y. V. Lobanov, F. S. Abdullin, A. N. Polyakov, R. N. Sagaidak, I. V. Shirokovsky, Y. S. Tsyganov, A. A. Voinov, G. G. Gulbekian, S. L. Bogomolov, B. N. Gikal, A. N. Mezentsev, S. Iliev, V. G. Subbotin, A. M. Sukhov, K. Subotic, V. I. Zagrebaev, G. K. Vostokin, M. G. Itkis *et al.*, Phys. Rev. C **74**, 044602 (2006).
[5] Y. T. Oganessian, F. S. Abdullin, C. Alexander, J. Binder, R. A. Boll, S. N. Dmitriev, J. Ezold, K. Felker, J. M. Gostic, R. K. Grzywacz, J. H. Hamilton, R. A. Henderson, M. G. Itkis, K. Miernik, D. Miller, K. J. Moody, A. N. Polyakov, A. V. Ramayya, J. B. Roberto, M. A. Ryabinin *et al.*, Phys. Rev. C **87**, 054621 (2013).
[6] B. M. Kayumov, O. K. Ganiev, A. K. Nasirov, and G. A. Yuldasheva, Phys. Rev. C **105**, 014618 (2022).
[7] M. Tanaka, P. Brionnet, M. Du, J. Ezold, K. Felker, B. J. Gall, S. Go, R. K. Grzywacz, H. Haba, K. Hagino, S. Hogle, S. Ishizawa, D. Kaji, S. Kimura, T. T. King, Y. Komori, R. K. Lemon, M. G. Leonard, K. Morimoto, K. Morita *et al.*, J. Phys. Soc. Jpn. **91**, 084201 (2022).
[8] Z.-H. Liu and J.-D. Bao, Phys. Rev. C **87**, 034616 (2013).
[9] A. K. Nasirov, G. Mandaglio, G. Giardina, A. Sobiczewski, and A. I. Muminov, Phys. Rev. C **84**, 044612 (2011).
[10] S. H. Zhu and X. J. Bao, Phys. Rev. C **108**, 014604 (2023).
[11] Y. T. Oganessian, V. K. Utyonkov, Y. V. Lobanov, F. S. Abdullin, A. N. Polyakov, R. N. Sagaidak, I. V. Shirokovsky, Y. S. Tsyganov, A. A. Voinov, A. N. Mezentsev, V. G. Subbotin, A. M. Sukhov, K. Subotic, V. I. Zagrebaev, S. N. Dmitriev, R. A. Henderson, K. J. Moody, J. M. Kenneally, J. H. Landrum, D. A. Shaughnessy *et al.*, Phys. Rev. C **79**, 024603 (2009).
[12] J. Khuyagbaatar, A. Yakushev, C. E. Düllmann, D. Ackermann, L.-L. Andersson, M. Asai, M. Block, R. A. Boll, H. Brand, D. M. Cox, M. Dasgupta, X. Derkx, A. Di Nitto, K. Eberhardt, J. Even, M. Evers, C. Fahlander, U. Forsberg, J. M. Gates, N. Gharibyan *et al.*, Phys. Rev. C **102**, 064602 (2020).
[13] S. Hofmann, S. Heinz, R. Mann, J. Maurer, S. Antalic, W. Barth, H. G. Burkhard, L. Dahl, and K. a. Eberhardt, Eur. Phys. J. A **52**, 180 (2016).
[14] Y. T. Oganessian, V. K. Utyonkov, Y. V. Lobanov, F. S. Abdullin, A. N. Polyakov, I. V. Shirokovsky, Y. S. Tsyganov, G. G. Gulbekian, S. L. Bogomolov, B. N. Gikal, A. N. Mezentsev, S. Iliev, V. G. Subbotin, A. M. Sukhov, A. A. Voinov, G. V. Buklanov, K. Subotic, V. I. Zagrebaev, M. G. Itkis, J. B. Patin *et al.*, Phys. Rev. C **70**, 064609 (2004).
[15] S. Hofmann, S. Heinz, R. Mann, J. Maurer, J. Khuyagbaatar, D. Ackermann, S. Antalic, W. Barth, M. Block, H. G. Burkhard *et al.*, Eur. Phys. J. A **48**, 62 (2012).
[16] S. Bjørnholm and W. Swiatecki, Nucl. Phys. A **391**, 471 (1982).
[17] V. Zagrebaev and W. Greiner, Nucl. Phys. A **944**, 257 (2015), Special Issue on Superheavy Elements.
[18] A. S. Umar, V. E. Oberacker, J. A. Maruhn, and P.-G. Reinhard, Phys. Rev. C **81**, 064607 (2010).
[19] M. Tohyama and A. S. Umar, Phys. Rev. C **93**, 034607 (2016).
[20] J.-X. Li and H.-F. Zhang, Phys. Rev. C **105**, 054606 (2022).
[21] G. Adamian, N. Antonenko, W. Scheid, and V. Volkov, Nucl. Phys. A **627**, 361 (1997).
[22] N. Wang, J.-q. Li, and E.-g. Zhao, Phys. Rev. C **78**, 054607 (2008).
[23] X. J. Bao, Y. Gao, J. Q. Li, and H. F. Zhang, Phys. Rev. C **91**, 011603(R) (2015).
[24] L. Zhu, W.-J. Xie, and F.-S. Zhang, Phys. Rev. C **89**, 024615 (2014).
[25] F. Li, L. Zhu, Z.-H. Wu, X.-B. Yu, J. Su, and C.-C. Guo, Phys. Rev. C **98**, 014618 (2018).
[26] G. Adamian, N. Antonenko, and Y. Tchuvil'sky, Phys. Lett. B **451**, 289 (1999).
[27] V. I. Zagrebaev, Y. Aritomo, M. G. Itkis, Y. T. Oganessian, and M. Ohta, Phys. Rev. C **65**, 014607 (2001).
[28] V. I. Zagrebaev, Phys. Rev. C **64**, 034606 (2001).
[29] V. I. Zagrebaev, Phys. Rev. C **67**, 061601(R) (2003).
[30] C. Y. Wong, Phys. Rev. Lett. **31**, 766 (1973).
[31] D. L. Hill and J. A. Wheeler, Phys. Rev. **89**, 1102 (1953).
[32] Z.-Q. Feng, G.-M. Jin, F. Fu, and J.-Q. Li, Nucl. Phys. A **771**, 50 (2006).
[33] W. D. Myers and W. J. Swiatecki, Nucl. Phys. **81**, 1 (1966).
[34] M. G. Itkis, G. N. Knyazheva, I. M. Itkis, and E. M. Kozulin, Eur. Phys. J. A **58**, 178 (2022).
[35] J.-X. Li and H.-F. Zhang, Phys. Rev. C **106**, 034613 (2022).
[36] J. Q. Li and G. Wolschin, Phys. Rev. C **27**, 590 (1983).
[37] J. D. Jackson, Can. J. Phys. **34**, 767 (1956).
[38] N. Bohr and J. A. Wheeler, Phys. Rev. **56**, 426 (1939).
[39] P. Möller, A. Sierk, T. Ichikawa, and H. Sagawa, At. Data Nucl. Data Tables **109–110**, 1 (2016).
[40] X. J. Bao, S. Q. Guo, H. F. Zhang, and J. Q. Li, Phys. Rev. C **96**, 024610 (2017).
[41] W. Loveland, Phys. Rev. C **76**, 014612 (2007).
[42] H. Lü, D. Boilley, Y. Abe, and C. Shen, Phys. Rev. C **94**, 034616 (2016).
[43] S. E. Agbemava, A. V. Afanasjev, D. Ray, and P. Ring, Phys. Rev. C **95**, 054324 (2017).
[44] S. Hofmann, J. Phys. G: Nucl. Part. Phys. **42**, 114001 (2015).